

Study of Laser Radiation Effect on the Cornea of the Eye by Speckle Interferometry

Victoria A. Fedulova, Aleksei V. Yuzhakov, and Olga I. Baum*

Federal Research Center “Crystallography and Photonics” of the Russian Academy of Sciences, 59 Leninskiy prospect, Moscow 119333, Russian Federation

* e-mail: baumolga@gmail.com

Abstract. The existing techniques of laser vision correction – one of the most widespread operations – are based presently on a surgical intervention in cornea tissue. Our science team is engaged in studying of in essence new type of correction based on a modification of structure and the field of mechanical tension of a cornea. In this work, the possibility to use of a speckle interferometry method as a basis for the tracking system of cornea structural changes at thermal influence of a nondestructive laser radiation is considered. Also for a cornea, the polymeric phantom was picked up. © 2020 Journal of Biomedical Photonics & Engineering.

Keywords: cornea; speckle interferometry method; polymeric phantom.

Paper #3350 received 30 Jan 2020; revised manuscript received 10 Mar 2020; accepted for publication 10 Mar 2020; published online 20 Mar 2020. [doi: 10.18287/JBPE20.06.010302](https://doi.org/10.18287/JBPE20.06.010302).

1 Introduction

The invention of lasers was a huge step forward for many fields of science. In medicine, lasers have become an important tool in oncology, dentistry, dermatology, surgery, and other fields. Currently, lasers have become very widespread in ophthalmology. According to the journal “Ophthalmology”, about 2 billion people suffer from myopia and this number will reach about 5 billion by 2050 [1]. In addition, serious concern is caused by the fact that problems with the visual system arise at an increasingly young age. So, among first graders, about 5% of children suffer from myopia, by the end of school this number increases to 25–30%, which contributes to the growing demand for vision correction.

Refractive surgery is based on changing the shape of the cornea – the anterior, most convex transparent part of the eyeball, one of the main refractor of the eye. It was previously believed that the cornea consists of 5 layers: the epithelium, the anterior border (Bowman) membrane, the stroma, the posterior border membrane (Desmetamen membrane) and the posterior epithelium (endothelium) [2]. However, in 2013, the sixth layer was discovered, which was called the Dua layer [3].

Now, changing the shape of the cornea is done by correcting the shape of the stroma that does not have the ability to regenerate. Different methods differ in various approaches to overcoming the epithelium and the Bowman membrane that can be restored after damage. Currently, several types of correction are distinguished:

PRK (photorefractive keratectomy), LASIK (Laser-Assisted in Situ Keratomileusis), LASEK (laser subepithelialkeratomileusis) [4], ReLEx SMILE [5].

The classical PRK method is as follows: after local anesthesia, de-epithelization is performed (mechanically, laser, or in another way), then the refraction stage itself is carried out (laser operation in the stroma), and, if necessary, the installation of protective lenses. Currently, a variant of photorefractive keratectomy, called trans-PRK, is a one-step technique that uses the cold ablation technique using an excimer laser.

PRK was recognized as the optimal method for the correction of mild and moderate myopia, however, with a high degree of myopia and astigmatism, the likelihood of postoperative complications and under correction is quite high. Besides, a sufficiently long recovery period causes certain inconveniences, as a result of which attempts to find another way of correction were not abandoned. LASIK was introduced in 1989. This type of correction allows you to work in deeper stroma layers. The innovation of LASIK consists in the formation of a corneal flap from the epithelial layers in the form of a circle connected to the rest of the cornea “leg” with a thickness of about 150 microns. Then the corneal flap rises and is laid aside to open the stromal zone of the cornea, on which the refractive stage of the operation itself is carried out. After changing the profile of the stroma, the epithelial flap returns to its place.

Modern vision correction technologies imply not only proper improvement of acuity and accommodation, but also an improvement in the quality of vision, as well as minimizing discomfort during and after surgery. A group of German ophthalmologists have developed the ReLEx method – Refractive Lenticule Extraction. At the moment, ReLEx SMILE is the only intrastromal corneal refractive laser operation performed without cutting out the surface corneal flap. The essence of the method is as follows: after local anesthesia, a lenticule is formed intrastromally, after that a small incision is made (from 2 to 4 mm). The lenticule is separated from the rest of the stroma by special tools, and then removed through the incision. The final step is washing the corneal pocket.

Due to the relatively recent introduction into practice, objective statistics for long-term follow-up of patients undergoing ReLEx SMILE do not yet exist, however, clinical data convincingly support this type of correction. The risk of postoperative complications is much lower than with other types of correction. It is obviously due to the smaller size of the dissection of biological tissue. In connection with these observations, it was concluded that it is necessary to introduce into the clinic a technique that does not violate the integrity of the biological tissues of the eye.

Our scientific group is studying a fundamentally new approach to the correction of refraction, based on the modification of cornea and sclera structure and their mechanical stresses field. The method consists of a combination of orthokeratology with laser radiation that does not damage the integrity of the eye tissue [6, 7]. Using a laser helps changing the conformation of collagen molecules located on the periphery of the cornea and in the limb. The method uses a special header that creates a circular distribution of the intensity of laser radiation [8–11], that allows us to achieve a more uniform effect of the weakening of mechanical stresses and leads to a reduction in laser-induced complications, since symmetric with respect to the paracentral zone cornea, but sequential irradiation of a number of points can lead to asymmetry of the corneal tension in the optical zone and the occurrence of astigmatism, keratoconus and other complications [8]. In addition, research is being carried out in the direction of developing a control system that allows one to determine the threshold for the onset of stress relaxation in the corneal tissues during laser irradiation. The studies are conducted in two different directions, one of which is based on optical coherent elastography [12–17], and the second direction is based on the speckle interferometry method, that the present work is devoted to.

2 MATERIALS AND METHODS

2.1 Eye tissue

The experiments were conducted *ex vivo* on pig eye samples. The extracted eyes were immediately frozen

and stored at a temperature of -4 to 10 °C. In preparation for the experiment, the eyes were thawed in physiological saline for 30 minutes at room temperature. Immediately before the experiment, the samples were removed from physiological saline and slightly dried in air to avoid absorption by excess water on the surface, and then placed in a special holder. All experiments were repeated at least 5 times.

2.2 Polyacrylamide hydrogels

In the mid 80s of the XX century, the widespread use of synthetic polymer materials for medical purposes began. Polymers and polymeric materials are used in various fields, for example, as diagnostic and therapeutic drugs (long-acting drugs, protecting tissues surrounding tumor from radiation, physiologically active polymers), anti-burn surgery, suture and dressings. However, the greatest distribution of polymeric materials was in plastic and reconstructive surgery.

In this work, we used polyacrylamide hydrogels (PAAG), which include acrylamide, NN'-methylenebisacrylamide, ammonium persulfate and TEMED (tetramethylethylenediamine).

The structure of acrylamide is as follows: $\text{CH}_2 = \text{CH} - \text{CONH}_2$. NN'-methylenebisacrylamide (Bisacrylamide) – $(\text{CH}_2 = \text{CH} - \text{CONH})_2 - \text{CH}_2 -$ acts as a “crosslinking” of linear acrylamide polymers. Ammonium persulfate is used to initiate the polymerization reaction (Fig. 1a). As a result of a homolytic rupture of the bond between oxygen atoms, two free radicals are formed (Fig. 1b) with a sufficiently long lifetime. The unpaired electron at the oxygen atom allows the radical to initiate the cleavage of the double bond in the acrylamide molecule and the formation of a new radical, in which the unpaired electron belongs to the carbon atom (Fig. 1c).

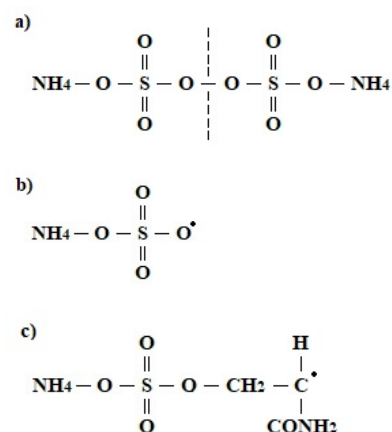


Fig. 1 The molecular structure of ammonium persulfate (a), free radical (b), and the combination of ammonium persulfate with acrylamide (c).

In turn, this radical is capable of causing a double bond in the next acrylamide molecule to break and to continue the polymerization chain reaction that ends

only after the two meets and the formation of the usual covalent bond.

One of the end groups of bisacrylamide can be integrated into the growing chain of a linear polymer. Its second end group may appear in another polymer chain, thus forming a crosslink – a bond between the polymer strands of acrylamide. The result of a large number of such bonds is a large branched network of hydrogel. TEMED is the catalyst for this process.

In this work, the main criteria for polyacrylamide hydrogels were the degree of crosslinking (determined by the ratio of acrylamide and bisacrylamide) and the percentage of the total mass of acrylamide and bisacrylamide to the volume of the solution. Based on the tabular data, a calculation was made for the intermediate values of these parameters. The necessary masses of substances included in the composition were measured on electronic scales, and then they were added to distilled water and mixed until completely dissolved. Then a catalyst (TEMED) was added to the solution and after that the hydrogel was collected in a syringe to give it a cylindrical shape convenient for research.

2.3 Speckle-Interferometry Method

Laser speckle-contrast technique (LSCI), due to its simplicity of execution, provides quick information on a wide area of motion of particles scattering light [18]. Over the past 15 years, it has become widely used as a tool for visualizing blood flow in the brain [19], skin [18], retina [20] and kidneys [21]. At the same time, the method itself continues to develop actively in terms of improving temporal and spatial resolutions, increasing the signal-to-noise ratio and searching for new applications [22–26].

The technique is based on the analysis of the speckle pattern arising as a result of random interference of coherent light scattered by a medium consisting of light-scattering particles. The motion of scattering particles leads to fluctuations in the interference pattern that can be recorded as changes in the intensity by the camera. Temporal and spatial statistics of the recorded speckle picture contains information about the movement. In particular, due to the finite integration time of the camera, motion will blur the speckle pattern, reducing speckle contrast.

The most common way to quantify blur is by calculating local speckle contrast [18, 19], that can be related to speed using autocorrelation functions of the field and intensity [19]. Theoretically, the contrast of a polarized speckle pattern takes values from 0 to 1 [27] (0 means that the scatters are fast enough to completely blur the speckle pattern, and 1 corresponds to a static, fully developed speckle pattern).

In this study, we used a LS-1.56 fiber laser (IPG Photonics Corp.) operating at a wavelength of 1.56 μm , with an output power of up to 5 W and the ability to control the duration of laser pulses and interpulse pauses. Irradiation mode: pulse-periodic mode, power density 15–56 W/cm^2 , exposure time 15 s, pulse duration and the interval between pulses 500 and

300 ms, respectively. The radiation was supplied through an optical fiber with a diameter of 600 μm , directed at an angle of 15° to the normal surface. Simultaneously with heating, the sample was illuminated with a wide beam of a helium-neon laser with an incidence angle of 45°. The probe beam reflected normally to the sample is detected by a 2D camera (Videozavr, VZ-M50S, 1296 × 972 pixels, 21 frames/s) to obtain an image and to monitor changes in the statistical properties of speckle patterns caused by heating. The surface temperature was monitored using an IR camera FLIR A615.

The obtained images were used to calculate the statistical functions of speckle patterns, such as the average light intensity, contrast (autocorrelation function), Pearson's cross-correlation coefficient (decorrelation function).

The average value of the intensity was calculated by the equation:

$$\langle I_k \rangle = \frac{1}{M * N} \sum_{m=1}^M \sum_{n=1}^N I_k, \quad (1)$$

where $\langle I_k \rangle$ is the average intensity value for frame k , I_k is the intensity value at the point of frame k with coordinates $\{m, n\}$, M is the width of the frame in pixels, N is the height of the frame in pixels.

To calculate the contrast function, we used the following relation:

$$V_k = \frac{\sigma_{I_k}}{\langle I_k \rangle} = \frac{\sqrt{\langle I_k \rangle^2 - \langle I_k^2 \rangle}}{\langle I_k \rangle}, \quad (2)$$

where V_k is the value of the contrast function calculated for each frame k .

The Pearson cross-correlation coefficient was calculated using the following equation:

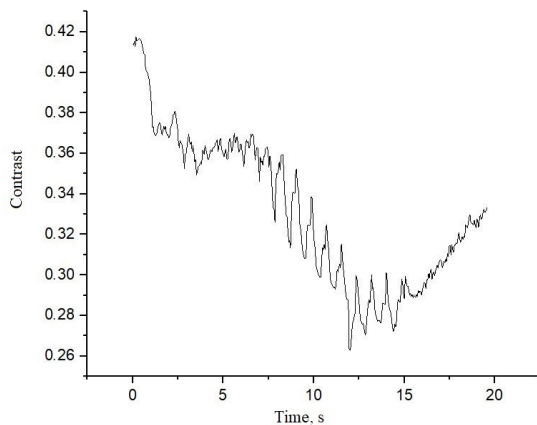
$$D_{k,l} = \frac{\text{cov}\langle I_k, I_l \rangle}{\sigma_{I_k} \sigma_{I_l}} = \frac{\langle I_k I_l \rangle - \langle I_k \rangle \langle I_l \rangle}{\sqrt{\langle I_k \rangle^2 - \langle I_k^2 \rangle} \sqrt{\langle I_l \rangle^2 - \langle I_l^2 \rangle}}, \quad (3)$$

where $D_{k,l}$ is the value of the cross-correlation Pearson coefficient calculated for each pair of frames k and l .

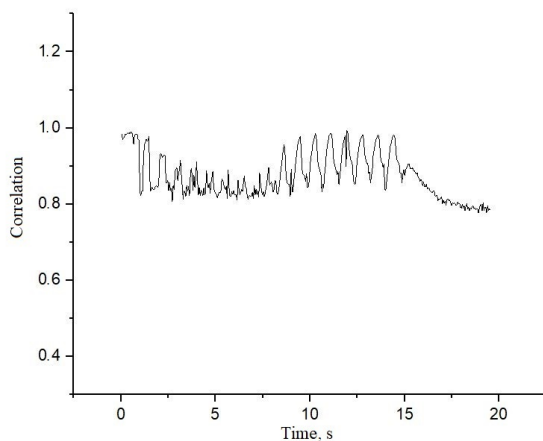
3 RESULTS AND DISCUSSION

The values of the contrast and correlation functions were measured for regions at the periphery and in the central part of the cornea for a pulse-periodic laser heating regime. On the graphs obtained, the denaturation moments are clearly visible, that can be determined by increasing the contrast graphs and by reducing the fluctuations of the correlation function. In the comparative graphs (Fig. 2), presenting the dependence of the contrast function and the correlation on time for the pulse-periodic mode, the motion of tissue inhomogeneities associated with its periodic

thermal expansion and contraction due to the laser operation mode is noted.



(a)



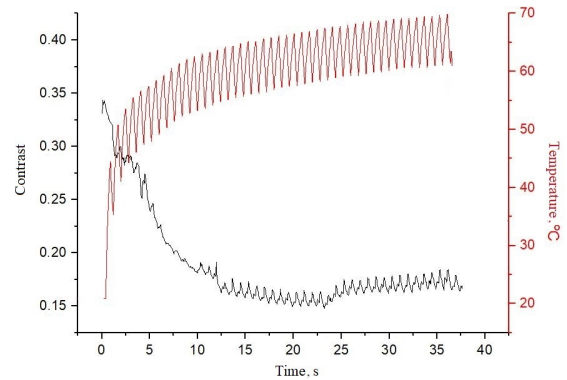
(b)

Fig. 2 Temporal dependences of contrast (a) and correlation coefficient (b) during heating of the cornea.

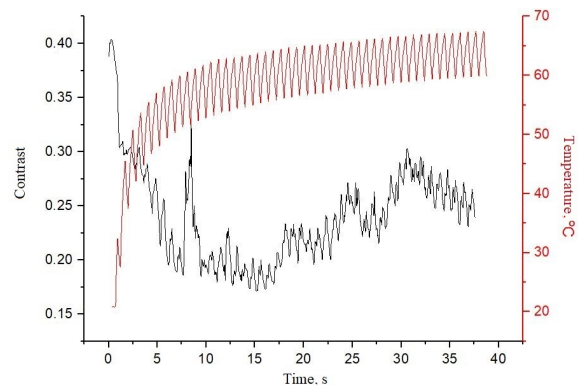
The oscillation amplitude of the contrast function for a region located in the central part of the cornea (Fig. 3a) is noticeably smaller compared to the oscillation amplitude for the periphery (Fig. 3b) that indicates a higher thermal resistance for central points. In the series of graphs obtained for the central part, the peaks of the contrast function are much less common than on the periphery, since when approaching the limb the stromal plates overlap each other that leads to the appearance of inhomogeneities associated with a violation of the parallelism of the collagen fibers.

Also graphs of the dependence of contrast on time were obtained for the regime that expects of stress relaxation. The biological tissue was irradiated for 20 sec (Fig. 4a), then it was soaked in saline for 5 min, and a 20 sec irradiation was repeated (Fig. 4b). The obtained graphs showed a qualitative similarity in the rate of decrease in the contrast function and the similarity of temperature profiles. The achieved maximum temperature also coincides, that allows us to

conclude that the thermomechanical characteristics of the cornea are restored. The variability of the results of repeated experiments is within 10% while maintaining the qualitative shape of the curves that indicates the potential use of this method as a control system.



(a)

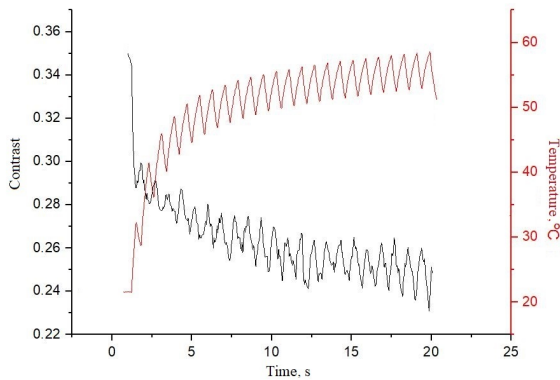


(b)

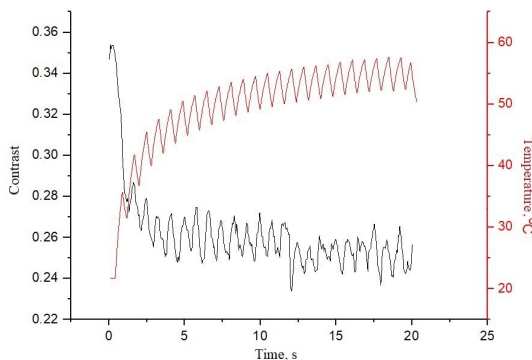
Fig. 3 Temporal dependences of contrast and temperature during pulse-periodic heating of the central (a) and peripheral (b) areas of the cornea.

A series of experiments was carried out for hydrogels with various degrees of crosslinking and the percentage of monomers in order to select a temperature profile that is most similar to the temperature profile obtained for the pig's cornea. The result of experiments series was the selection of the hydrogel composition with the temperature profile (Fig. 5a) similar to the temperature profile of the cornea. The composition of the obtained hydrogel includes Acrylamide – 0.2 g; Bisacrylamide – 0.0222 g; Ammonium persulfate – 0.0005 g; TEMED – 0.0001 g; Distilled water - 2 ml. The crosslinking degree of this hydrogel is 1:19, the percentage of monomers is 10%. At the same percentage of monomers, but with a lower degree of crosslinking (1:9), a noticeable similarity of temperature profiles is observed, but after about 25 sec of irradiation, the graphs begin to diverge (Fig. 5b). When the degree of crosslinking is 1:19 and the percentage of

monomers is 30%, the temperature profiles do not coincide.



(a)



(b)

Fig. 4 Temporal dependences of contrast and temperature during initial (a) and repeated (b) pulse-periodic heating of the cornea.

In the future, it will be used for the manufacture of phantoms for studies of thermal conductivity and the selection of optimal laser irradiation modes for various irradiation geometry.

4 Conclusion

In this work, a PAAG was selected with the temperature profile corresponded to the temperature profile of the cornea under pulse-periodic laser heating.

It was shown that the time and temperature dependences of the contrast and correlation functions make it possible to track the onset of structural changes in the corneal tissues during pulse-periodic laser heating. The difference in the behavior of these curves for the central and peripheral areas of the cornea is shown.

The obtained results and their repeatability allow us to conclude that it is possible to use the speckle interferometry method as a basis for a system for monitoring of the structural changes in the cornea associated with the thermal effect of laser radiation. The method requires further tuning to more clearly present

the results of the experiment, but the qualitative similarity of the obtained graphs and the ability to track the moments of denaturation prove the feasibility of its development.

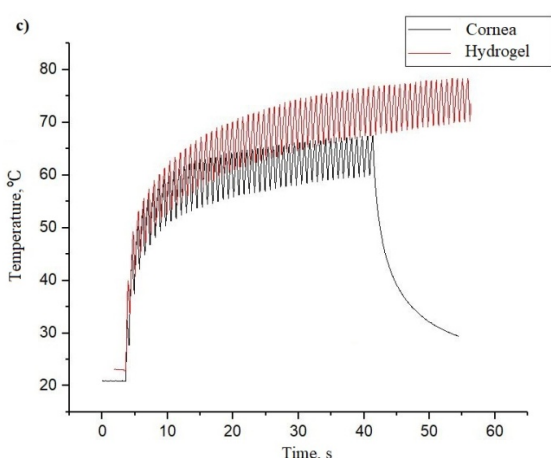
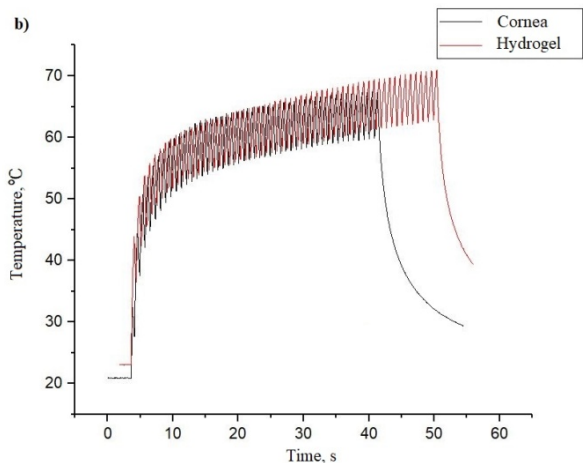
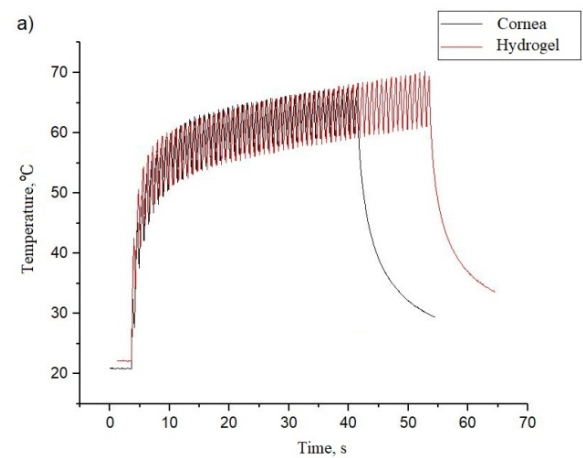


Fig. 5 Temperature profiles of the cornea and PAAG: a) the degree of crosslinking 1:19, the percentage of monomers 10%; b) the degree of crosslinking 1:9, the percentage of monomers 10%; c) the degree of crosslinking 1:19, the percentage of monomers 30%.

Disclosures

All authors declare that there is no conflict of interests in this paper.

Acknowledgments

This work was supported by the Ministry of Science and Higher Education of Russian Federation within the State assignment FSRC «Crystallography and Photonics» RAS.

References

1. B. A. Holden, T. R. Fricke, D. A. Wilson, M. Jong, K. S. Naidoo, P. Sankaridurg, T. Y. Wong, T. J. Naduvilath, and S. Resnikoff, “[Global Prevalence of Myopia and High Myopia and Temporal Trends from 2000 through 2050](#),” *Ophthalmology* 123(5), 1036–1042 (2016).
2. K. E. Johnson, *Histology and cell biology*, Williams & Wilkins, Baltimore, Maryland (1991).
3. H. S. Dua, L. A. Faraj, D. G. Said, T. Gray, and J. Lowe, “[Human Corneal Anatomy Redefined](#),” *Ophthalmology* 120(9), 1778–1785 (2013).
4. S. Taneri, J. D. Zieske, and D. T. Azar, “[Evolution, techniques, clinical outcomes, and pathophysiology of LASEK: review of the literature](#),” *Survey of Ophthalmology* 49(6), 576–602 (2004).
5. W. Sekundo, J. Gertner, T. Bertelmann, and I. Solomatin, “[One-year refractive results, contrast sensitivity, high-order aberrations and complications after myopic small-incision lenticule extraction \(ReLExSMILE\)](#),” *Graefes’ Archive for Clinical and Experimental Ophthalmology* 252(5), 837–843 (2014).
6. E. N. Sobol’, O. I. Baum, A. V. Bol’shunov, V. I. Siplivy, N. Y. Ignat’eva, O. L. Zakharkina, V. V. Lunin, A. I. Omelchenko, V. A. Kamensky, and A. V. Mjakov, “[Eye Tissue Structure and Refraction Variations upon Nondestructive Laser Action](#),” *Laser Physics* 16(5), 735–740 (2006).
7. A. Bolshunov, E. Sobol, S. Avetisov, O. Baum, V. Siplivy, and A. Omelchenko, “[A new method of the eye refraction correction under nonablative laser radiation](#),” *ActaOphthalmologica* 89 (2011).
8. O. I. Baum, A. V. Yuzhakov, A. V. Bolshunov, V. I. Siplivyi, and O. V. Khomchik, “[New laser technologies in ophthalmology for normalisation of intraocular pressure and correction of refraction](#),” *Quantum electronics* 47(9), 860 (2017).
9. O. Baum, A. Yuzhakov, A. Omelchenko, A. Bolshunov, V. Siplivy, and E. Sobol, “[Laser-assisted correction of eye cornea refraction with ring-shaped laser beam](#),” *Proceedings of SPIE* 104170, 104170H (2017).
10. O. I. Baum, A. I. Omelchenko, E. M. Kasyanenko, R. V. Skidanov, and N. L. Kazanskij, “[New biophotonics methods for improving efficiency and safety of laser modification of the fibrous tunic of the eye](#),” *Vestnik oftalmologii* 134(5), 4–14 (2018).
11. O. I. Baum, A. I. Omel’chenko, E. M. Kasianenko, R. V. Skidanov, N. L. Kazanskiy, A. V. Bolshunov, S. E. Avetisov, and V. Y. Panchenko, “[Control of laser-beam spatial distribution for correcting the shape and refraction of eye cornea](#),” *Quantum Electronics* 50(1), 87 (2020).
12. O. I. Baum, V. Y. Zaitsev, A. V. Yuzhakov, A. P. Sviridov, M. L. Novikova, A. L. Matveyev, L. A. Matveev, A. A. Sovetsky, and E. N. Sobol, “[Interplay of temperature, thermal - stresses and strains in laser - assisted modification of collagenous tissues: Speckle - contrast and OCT - based studies](#),” *Journal of Biophotonics* 13(1), e201900199 (2019).
13. V. Y. Zaitsev, A. L. Matveyev, L. A. Matveev, G. V. Gelikonov, A. Vitkin, A. I. Omelchenko, O. I. Baum, D. V. Shabanov, A. A. Sovetsky, and E. N. Sobol, “[Multiparameter thermo-mechanical OCT-based characterization of laser-induced cornea reshaping](#),” *Proceedings of SPIE* 10067, 100670V (2017).
14. V. Y. Zaitsev, A. L. Matveyev, L. A. Matveev, G. V. Gelikonov, O. I. Baum, A. I. Omelchenko, D. V. Shabanov, A. A. Sovetsky, A. V. Yuzhakov, A. A. Fedorov, V. I. Siplivy, A. V. Bolshunov, and E. N. Sobol, “[Revealing structural modifications in thermomechanical reshaping of collagenous tissues using optical coherence elastography](#),” *Journal of biophotonics* 12 (3), e201800250 (2019).
15. V. Y. Zaitsev, L. A. Matveev, A. L. Matveyev, A. A. Sovetsky, D. V. Shabanov, S. Y. Ksenofontov, G. V. Gelikonov, O. I. Baum, A. I. Omelchenko, A. V. Yuzhakov, and E. N. Sobol, “[Optimization of phase-resolved optical coherence elastography for highly-sensitive monitoring of slow-rate strains](#),” *Laser Physics Letters* 1(6), 065601 (2019).
16. V. Y. Zaitsev, A. L. Matveyev, L. A. Matveev, G. V. Gelikonov, A. Vitkin, A. I. Omelchenko, O. I. Baum, D. V. Shabanov, A. A. Sovetsky, and E. N. Sobol, “[Multiparameter thermo-mechanical OCT-based characterization of laser-induced cornea reshaping](#),” *Proceedings of SPIE* 10067, 100670V (2017).
17. V. Y. Zaitsev, A. L. Matveyev, L. A. Matveev, G. V. Gelikonov, A. I. Omelchenko, D. V. Shabanov, A. A. Sovetsky, O. I. Baum, A. Vitkin, and E. N. Sobol, “[Optical coherence elastography assesses tissue modifications in laser reshaping of cornea and cartilages](#),” *Proceedings of SPIE* 10496, 104960C (2018).

18. D. Briers, D. D. Duncan, E. Hirst, S. J. Kirkpatrick, M. Larsson, W. Steenbergen, T. Stromberg, and O. B. Thompson, “[Laser speckle contrast imaging: theoretical and practical limitations](#),” *Journal of Biomedical Optics* 18(6), 066018 (2013).
19. D. A. Boas, A. K. Dunn, “[Laser speckle contrast imaging in biomedical optics](#),” *Journal of Biomedical Optics* 15(1), 011109 (2010).
20. A. Y. Neganova, D. D. Postnov, J. C. B. Jacobsen, and O. Sosnovtseva, “[Laser speckle analysis of retinal vascular dynamics](#),” *Biomedical Optics Express* 7(4), 1375–1384 (2016).
21. D. D. Postnov, N.-H. Holstein-Rathlou, and O. Sosnovtseva, “[Laser speckle imaging of intra organ drug distribution](#),” *Biomedical Optics Express* 6(12), 5055–5062 (2015).
22. A. S. Abdurashitov, V. V. Lychagov, O. A. Sindeeva, O. V. Semyachkina-Glushkovskaya, and V. V. Tuchin, “[Histogram analysis of laser speckle contrast image for cerebral blood flow monitoring](#),” *Frontiers of Optoelectronics* 8(2), 187–194 (2015).
23. D. D. Postnov, O. Sosnovtseva, and V. V. Tuchin, “[Improved detectability of microcirculatory dynamics by laser speckle flowmetry](#),” *Journal of Biophotonics* 8(10), 790-794 (2015).
24. D. D. Postnov, V. V. Tuchin, and O. Sosnovtseva, “[Estimation of vessel diameter and blood flow dynamics from laser speckle images](#),” *Biomed. Optics Express* 7(7), 2759–2768 (2016).
25. A. Abdurashitov, O. Bragina, O. Sindeeva, S. Sindeev, O. V. Semyachkina-Glushkovskaya, and V. V. Tuchin, “[Off-axis holographic laser speckle contrast imaging of blood vessels in tissues](#),” *Journal of Biomedical Optics* 22(9), 091514 (2017).
26. Z. Hajjarian, H. T. Nia, S. Ahn, A. J. Grodzinsky, R. K. Jain, and S. K. Nadkarni, “[Laser speckle rheology for evaluating the viscoelastic properties of hydrogel scaffolds](#),” *Scientific Reports* 6(1), 37949 (2016).
27. D. D. Duncan, S. J. Kirkpatrick, and R. K. Wang, “Statistics of local speckle contrast,” *Journal of the Optical Society of America A* 25(1), 9–15 (2008).